Tellus (1995), 47A, 365–382
Printed in Belgium 


TELLUS
ISSN 0280–6495

# Use of the flow relaxation scheme in a three-dimensional baroclinic ocean model with realistic topography

By HARALD ENGEDAHL, *The Norwegian Meteorological Institute (DNMI), P.O. Box 43 Blindern, N-0313 Oslo, Norway*

(Manuscript received 1 December 1992; in final form 9 May 1994)

ABSTRACT

A three-dimensional numerical ocean model was set up for a domain covering the Nordic Seas to produce dynamically consistent climatological archives of sea level, current, salinity and temperature. The flow relaxation scheme (FRS) was applied as open boundary condition. As a first step the model was run in *diagnostic* mode until a stationary solution was obtained. The only forcing was provided by gridded climatological fields of salinity and temperature. Compared with available data, this model set up produced a satisfactory circulation in the Nordic Seas. The results were stored in *The Diagnostic Archive*. In the next step, the obtained stationary solutions were used as boundary values in *prognostic* simulations to produce *The Prognostic Archive*. This paper describes a method for handling open boundary conditions in *diagnostic* simulations. The method requires knowledge of the depth mean current. A rather artificial condition of zero depth mean current or transport was chosen. Because the FRS does not conserve mass or momentum, it is able to redistribute the specified zero transports to nonzero in a realistic way through the relaxation zones. However, if the open boundaries are situated in dynamical active areas, in which contour lines of $f/H$ enter or leave the model domain, the production of nonzero transports in the FRS zones is not sufficient to provide satisfactory boundary conditions. Instead, if already computed sea level and currents from a simulation with a larger model domain are used as external solutions at the open boundaries, the model gives excellent results. To illustrate the performance of the FRS when the temperature and salinity fields also are allowed to evolve, i.e., *prognostic* simulation, an example is shown from *The Prognostic Archive*. Here, boundary values were extracted from *The Diagnostic Archive*.

## 1. Introduction

In the last few years, an increasing attention has been drawn towards the use of regional numerical ocean models for simulating climatological circulation patterns in the ocean. There is a growing consensus that the key to understand the present climatic conditions, and be able to predict possible future changes over several decades, to a large degree is hidden in a better understanding of the dynamics in the ocean. At mid-latitudes on the northern hemisphere the inflow of warm Atlantic water of equatorial origin (The Gulf Stream) into the area denoted as the Nordic Seas, is the most dominant factor that influences the local climate. The Nordic Seas is the ocean area limited in the south by the submarine ridge from Greenland, across Iceland to The Faroes and Scotland, and in the north by the Fram Strait. It appears that the Nordic Seas is a very sensitive region, and that a better knowledge of the processes in these areas may by essential for understanding the global changes in climate.

Several numerical studies of the dynamics in the Nordic Seas have been performed. Legutke (1991) studied the effects of seasonal wind forcing on the circulation in the Greenland and Norwegian Seas with a primitive equation numerical model using a horizontal resolution of approximately 20 km. Climatological data from the global data base of Levitus (1982) was used as initial conditions regarding salinity and temperature. Open lateral boundaries were located in dynamically active areas, where the volume exchanges were explicitly described. The produced circulation seemed to be trapped by closed contour lines of $f/H$, i.e., topography is important, and the currents were essentially depth independent. The velocities and transports produced by the model showed reasonable agreement with observed values. A quite similar study was performed by Stevens (1991). In this study the numerical model was forced by annual mean and seasonally varying wind and thermohaline forcing through prescribed surface values of salinity and temperature. The grid resolution was approximately 55 km. Again, the results indicated that the effect of topography is very important. Many of the observed features of the temperature and salinity fields as well as currents were reproduced.

Since the Nordic Seas seems to be a very interesting area as far as climatological changes are concerned, a digitized climatological data base containing monthly mean sea surface elevation, currents, salinity and sea temperature should provide a very useful aid for further investigations in that area. Because of the present computer capacity the ocean models used for studies of the circulation in the Nordic Seas have a limited horizontal grid resolution, usually between 20 and 100 km. This is sufficient to resolve the barotropic response, with a length scale from 100 km and above, while the baroclinic response is poorly resolved, if at all. The baroclinic Rossby radius in the actual area is between 10 and 30 km, depending on the stratification. Thus, features such as baroclinic mesoscale eddies are not resolved at all. However, for *diagnostic* simulations, in which the imposed fields of salinity and temperature are kept constant in time, a horizontal resolution of 20 km should be sufficient to resolve the most important features of the oceanic circulation. The available salinity and temperature fields very often originate from climatological data bases with rather coarse horizontal resolution.

In fact, the presented study arose from the work of creating dynamically consistent digitized data bases containing monthly mean fields of sea level, currents, salinity and temperature for the Nordic Seas. To achieve this, a three-dimensional primitive equation numerical ocean model was applied. This model is originally developed at the University of Princeton, and denoted the Princeton Ocean Model (POM) or the Estuarine Circulation Ocean Model (ECOM-3D) (Blumberg and Mellor, 1987). The horizontal resolution was 20 km. On the basis of experience and several earlier studies, the dynamics in the Nordic Seas are controlled by atmospheric forcing, thermohaline forcing through surface fluxes of salinity and temperature, topography, river run off or fresh water discharge, and driving forces specified at the open boundaries.

The climatological archives were produced in two steps. As a first step, the model was set up for a large area and run in diagnostic mode until a stationary circulation was obtained. By running the model in diagnostic mode, the fields of salinity and temperature were kept constant in time. As initial condition climatological salinity and temperature fields were taken from the global hydrographical data base of Levitus (1982). For the North Sea, finer resolution data from Damm (1989) was applied. The only forcing of the model consisted of the imposed climatological density field derived from the data of Levitus (1982) and Damm (1989), together with the specified values of surface elevation and current at the open boundaries. This was done for every month producing a first order archive (Diagnostic Archive) for sea level and current based on the climatological fields of salinity and temperature. In these diagnostic runs rather simple boundary conditions for sea level and current were applied. The depth integrated current or transport was zero along the open boundaries, while the current at each level was computed from the thermal wind equations. The sea level was found from geostrophic balance with the computed current in the upper level. This paper focus on the work connected to the handling of the open boundaries in *diagnostic* simulations.

The next step in the process of creating dynamically consistent climatological archives, also including adjusted fields of salinity and temperature, was to run the model prognostically on a smaller domain embedded in the domain for the diagnostic simulations. Here, the fields of salinity and temperature were allowed to evolve, and boundary values for sea level and current were extracted from The Diagnostic Archive. In addition, monthly mean winds and fresh water discharge together with the $M_2$ tide were included. The model was run for several years to obtain a consistent seasonal variation. An example from this Prognostic Archive is given in Subsection 5.3.

By this two-step method, one obtains a significant enhancement of the circulation produced in the prognostic runs, compared to the results in The Diagnostic Archive, which were applied as boundary values. By reducing the model domain relative to that in The Diagnostic Archive, the flux of salinity and temperature at the boundaries are also improved because of the nonzero transports allowed by the applied boundary condition inside of the boundaries of The Diagnostic Archive.

As mentioned by both Legutke (1991) and Stevens (1991) open boundaries, which naturally occur in *regional* ocean models, are often difficult to handle. Dynamical variables such as sea surface elevation and volume transports are very often directly specified along the open boundaries in dynamically active areas. Here, instead of using a similar procedure, the flow relaxation scheme (FRS) (Davies, 1976; Kållberg and Gibson, 1977; Martinsen and Engedahl, 1987) was applied as the open boundary condition. Using the FRS, the solution near the boundary is relaxed towards an exterior specified solution, and the model equations themselves will control the circulation in the vicinity of the open boundaries. Because observations of the prognostic variables are sparse, and the available data contain a lot of uncertainties, the use of the FRS should provide an alternative to the many different approaches in connection with the specification of boundary values in regional ocean models. Similar relaxation methods have already been successfully used in regional atmospheric numerical models for some time (Davies, 1983), and the FRS is at present used in the regional atmospheric prediction model at DNMI. The FRS has also been applied in the operational two-dimensional storm surge forecast model at DNMI, and is presently used in the ECOM-3D model for operational forecasts of currents. It may be mentioned that the FRS was also used by Cooper and Thompson (1989) in modelling hurricane induced currents in the Gulf of Mexico, and by Hannah et al. (1991) for studying tidally forced motion on the west coast of Canada.

A brief description of the numerical model is contained in Section 2. The FRS is described in Section 3. A simple method for specification of boundary values of velocity and sea level is outlined in Section 4. Description of the different numerical experiments and discussion of the results are contained in Section 5. Section 6 yields a summary and the final conclusions.

## 2. The numerical model

The basic equations of the model describe the velocity field, the surface elevation and the salinity and temperature fields. The following two simplifying approximations are used. First, it is assumed that the weight of the fluid identically balances the pressure, i.e., the *hydrostatic approximation*, and second, density variations are neglected unless the density is multiplied by gravity, i.e., the *Boussinesq approximation*.

In *diagnostic mode*, the following equations are applied. Consider a system of orthogonal Cartesian coordinates with $x$, $y$ and $z$ (increasing upward). Then, the free surface is located at $z=\eta(x, y, t)$ and the bottom at $z=-H(x, y)$. The continuity equation is

$$\nabla \cdot \boldsymbol{v} + \frac{\partial w}{\partial z} = 0, \tag{2.1}$$

where $\boldsymbol{v}$ is the horizontal velocity vector with components $(u, v)$, $w$ is the vertical velocity component and $\nabla$ is the horizontal gradient operator. The Reynolds momentum equations (with hydrostatic and Boussinesq approximations included) are:

$$\frac{\partial u}{\partial t} + \boldsymbol{v} \cdot \nabla u + w\frac{\partial u}{\partial z} - fv = -\frac{1}{\rho_0}\frac{\partial p}{\partial x} + \frac{\partial}{\partial z}\left(K_M \frac{\partial u}{\partial z}\right) + F_x, \tag{2.2}$$

$$\frac{\partial v}{\partial t} + \boldsymbol{v} \cdot \nabla v + w\frac{\partial v}{\partial z} + fu = -\frac{1}{\rho_0}\frac{\partial p}{\partial y} + \frac{\partial}{\partial z}\left(K_M \frac{\partial v}{\partial z}\right) + F_y. \tag{2.3}$$

In the vertical we have:

$$\rho g = -\frac{\partial p}{\partial z}. \tag{2.4}$$

Here, $\rho_0$ is the reference density, $\rho$ the actual density, $f$ the Coriolis parameter, $g$ the gravitational acceleration, $p$ the pressure and $K_M$ the vertical mixing coefficient for momentum.

The conservation equations for temperature and salinity are not active in diagnostic mode. Using the prescribed temperature $\theta$ and the salinity $S$, the density is computed according to an equation of state of the form

$$\rho = \rho(\theta, S). \tag{2.5}$$

The terms $F_x, F_y$ in the momentum equations represent unresolved horizontal mixing processes, and in analogy with molecular diffusion they are written as

$$F_x = \frac{\partial}{\partial x}\left(2A_M \frac{\partial u}{\partial x}\right) + \frac{\partial}{\partial y}\left(A_M\left(\frac{\partial u}{\partial y} + \frac{\partial v}{\partial x}\right)\right), \tag{2.6}$$

$$F_y = \frac{\partial}{\partial y}\left(2A_M \frac{\partial v}{\partial y}\right) + \frac{\partial}{\partial x}\left(A_M\left(\frac{\partial u}{\partial y} + \frac{\partial v}{\partial x}\right)\right). \tag{2.7}$$

The horizontal diffusivity $A_M$ is usually required to damp small scale noise due to the energy cascade. In this model the horizontal mixing coefficient depends on the horizontal velocity shear and on the grid spacing in the following manner (Smagorinsky, 1963):

$$A_M = C\,\Delta x\,\Delta y\left[\left(\frac{\partial u}{\partial x}\right)^2 + \frac{1}{2}\left(\frac{\partial v}{\partial x} + \frac{\partial u}{\partial y}\right)^2 + \left(\frac{\partial v}{\partial y}\right)^2\right]^{1/2}. \tag{2.8}$$

The vertical mixing coefficient, $K_M$ in the momentum equations was calculated by using a second order turbulence closure sub-model (Mellor and Yamada, 1982). This sub-model characterizes the turbulence by prognostic equations for the turbulent kinetic energy ($q^2$), and the turbulent macroscale ($l$). The details of the closure model are rather involved, but it is possible to prescribe the mixing coefficient $K_M$ in the following way:

$$K_M \equiv lqS_M. \tag{2.9}$$

Here, the stability function $S_M$ is an analytically derived, algebraic relation functionally dependent on $\partial u/\partial z$, $\partial v/\partial z$, $\partial \rho/\partial z$, $q$ and $l$.

In the numerical approach, a terrain following vertical coordinate $\sigma$ is introduced, i.e., the vertical coordinate is scaled by the water column depth:

$$\sigma = \frac{z - \eta}{\eta + H}. \tag{2.10}$$

Furthermore, the same numerical approach as described in Blumberg and Mellor (1987) was applied.

## 3. The flow relaxation scheme (FRS)

The flow relaxation scheme (FRS) (Davies, 1976; Kållberg and Gibson, 1977; Martinsen and Engedahl, 1987) was implemented as an open boundary condition in the numerical model. This scheme was originally designed to relax external solutions from a large area model towards solutions in a limited area model with a finer grid resolution, i.e., nesting. The relaxation takes place within specified marginal zones applied along the open boundaries; hereafter denoted FRS zones. The FRS has been used for some years in regional numerical atmospheric models; see Davies (1976, 1983), Kållberg and Gibson (1977). In the last few years it has also been applied in several numerical ocean models; see Martinsen and Engedahl (1987), Cooper and Thompson (1989) and Hannah et al. (1991).

### *3.1. Method*

Let $\varphi_i$ be any prognostic variable calculated in the interior of the model domain. Then in the FRS zones the variables are redefined or relaxed by the following equation:

$$\varphi = \alpha\varphi_e + (1 - \alpha)\,\varphi_i. \tag{3.1}$$

Here, $\varphi_e$ is the external solution and $\varphi$ is the new updated value in the FRS zones. The relaxation parameter $\alpha$ varies between 0 and 1 within the relaxation zones. It is equal to 1 at the outer ends of the zones, which involves that here $\varphi = \varphi_e$, and decreases smoothly towards 0 at the inner ends where $\varphi = \varphi_i$. When the external solution is set to a *constant*, the FRS method degenerates to a sponge type open boundary condition (Martinsen and Engedahl, 1987).

### *3.2. Some properties of the FRS*

The FRS has shown to have the ability of filtering noise from the external solution through the FRS zones, and leave the internal solution almost undisturbed both at the inflow and outflow boundaries (Martinsen and Engedahl, 1987). For instance, noise in observed or measured fields which are used as boundary values or external solutions, should be filtered by the FRS. However, the physical nature of the external solution should not differ significantly from the expected solution in the model domain if the FRS shall be able to work properly as open boundary condition. This is further discussed below and illustrated in Subsection 5.2.2.

The use of the FRS implies introduction of *overspecified* boundary fields. Because of this, a damping mechanism must be applied to remove spurious waves. By using the FRS, the necessary damping is implicitly induced as a Newtonian friction in the FRS zones; see Martinsen and Engedahl (1987). Another property of the FRS is that it does not conserve mass and momentum. As a consequence, zero external solutions are transferred or redistributed to nonzero through the FRS zones. This may be exploited if the external solutions are unknown and put equal to zero, as discussed in Section 5. The fact that the FRS does not conserve vorticity was pointed out by Davies (1976). Regarding divergence, it is easy to show that the variation of $\alpha$ together with the difference between the external and internal solutions acts to produce artificial divergence in the FRS zones. This may be demonstrated by considering the vertically integrated continuity equation, which may be written:

$$\frac{\partial \eta}{\partial t} = -\left(\frac{\partial U}{\partial x} + \frac{\partial V}{\partial y}\right) \equiv -\delta, \tag{3.2}$$

where $U$ and $V$ are the volume fluxes in the $x$- and $y$-direction, respectively. The divergence is denoted by $\delta$. In the FRS zones all prognostic variables are relaxed by (3.1). Inserting for $\eta$, $U$ and $V$ in (3.2) using (3.1) gives:

$$\begin{aligned}\frac{\partial}{\partial t}(\alpha\eta_e + (1-\alpha)\eta_i) &= -\left\{\alpha\frac{\partial U_e}{\partial x} + U_e\frac{\partial \alpha}{\partial x} + \frac{\partial U_i}{\partial x} - \alpha\frac{\partial U_i}{\partial x} - U_i\frac{\partial \alpha}{\partial x}\right.\\ &\left.+\alpha\frac{\partial V_e}{\partial y} + V_e\frac{\partial \alpha}{\partial y} + \frac{\partial V_i}{\partial y} - \alpha\frac{\partial V_i}{\partial y} - V_i\frac{\partial \alpha}{\partial y}\right\}.\end{aligned} \tag{3.3}$$

Eq. (3.3) may be written as:

$$\begin{aligned}\alpha\frac{\partial \eta_e}{\partial t} + (1-\alpha)\frac{\partial \eta_i}{\partial t} &= -\{\alpha\,\delta_e + (1-\alpha)\,\delta_i\}\\ &+\left\{(U_e - U_i)\frac{\partial \alpha}{\partial x} + (V_e - V_i)\frac{\partial \alpha}{\partial y}\right\},\end{aligned} \tag{3.4}$$

where

$$\begin{aligned}\delta_e &\equiv \frac{\partial U_e}{\partial x} + \frac{\partial V_e}{\partial y},\\ \delta_i &\equiv \frac{\partial U_i}{\partial x} + \frac{\partial V_i}{\partial y}.\end{aligned} \tag{3.5}$$

Eq. (3.4) is the continuity equation in the FRS zones (a similar procedure may be applied for the vorticity). Compared with (3.2), we now have two additional terms on the right hand side. These terms contain the products of the difference between the external and internal (or unrelaxed) solution and the horizontal derivatives of $\alpha$. Thus, the production of artificial divergence is equally dependent on two factors: (1) How smooth $\alpha$ is distributed in the FRS zones, and (2) The difference between the external and internal solutions. A smoother distribution of $\alpha$ may be obtained by specifying wider FRS zones. However, this will require more computer memory and be more computer demanding. From eq. (3.4) we see that if we are able to specify a "correct" external solution, so that $U_e = U_i$ and $V_e = V_i$, the FRS will conserve the divergence in the FRS zones *independent* of the distribution of $\alpha$. The importance of specifying "correct" external solutions is elucidated in Subsection 5.2.2.

## 4. Boundary values for current and sea level

In this section, we describe a simple method to produce boundary values for the sea surface elevation $\eta$ and the depth dependent velocities $u$ and $v$. These values are then used as external solutions in the FRS zones along the open boundaries of the model domain.

Since climatological three-dimensional fields of salinity and temperature already were available from a gridded data archive, it was naturally to try to determine velocities and surface elevation based on those fields. The gridded data archive was based on two climatological data sets originating from Levitus (1982) and Damm (1989). The data from Levitus cover the entire world ocean, however, the data have the disadvantage of being rather smooth. Because of this, the data from Damm were merged with the data of Levitus. The data of Damm have a much higher resolution than the data from Levitus, but Damm's data only cover the North Sea and the Skagerak. The griding procedure of the climatological data from Levitus and Damm is described in Martinsen et al. (1992). The gridded data archive contains monthly mean values of salinity and temperature fields at the standard oceanographic depths from sea surface down to 5500 m, covering an area slightly larger than the largest model domain shown in Fig. 1. In this study, the selected salinity and temperature fields were valid for the month of February. Thus, the resulting circulation produced by the numerical model should be valid for the winter season.

The density $\rho = \rho(x, y, z)$ is easily computed for the entire model domain and at each standard oceanographic level from the equation of state (2.5). By assuming geostrophic balance and stating the "thermal wind equations"

$$\frac{\partial u}{\partial z} = \frac{g}{\rho_0 f} \frac{\partial \rho}{\partial x}, \tag{4.1}$$

$$\frac{\partial v}{\partial z} = -\frac{g}{\rho_0 f} \frac{\partial \rho}{\partial y}, \tag{4.2}$$

it is possible to compute the vertical gradients of the velocities $\partial u/\partial z$ and $\partial v/\partial z$, at each level.

The velocities may then be written as

$$u = \int \frac{\partial u}{\partial z} dz + u_m - \frac{1}{H} \int_{-H}^{0} \left( \int \frac{\partial u}{\partial z} dz \right) dz, \tag{4.3}$$

$$v = \int \frac{\partial v}{\partial z} dz + v_m - \frac{1}{H} \int_{-H}^{0} \left( \int \frac{\partial v}{\partial z} dz \right) dz. \tag{4.4}$$

The depth mean integrated velocities $u_m$ and $v_m$ are computed as

$$u_m = \frac{1}{H} \int_{-H}^{0} u \, dz, \tag{4.5}$$

$$v_m = \frac{1}{H} \int_{-H}^{0} v \, dz. \tag{4.6}$$

Here, we assume that $\eta \ll H$.

*Numerically*, from (4.1) and (4.2) $\partial u/\partial z$ and $\partial v/\partial z$ can only be computed at the *discrete levels* at which we know the density. Between these levels, we assume that the velocities vary *linearly* with depth. Thus, $\partial u/\partial z$ and $\partial v/\partial z$ are both assumed to be constant with depth between each level. Because of this, we are able to easily compute the integrals on the right hand side in (4.3) and (4.4).

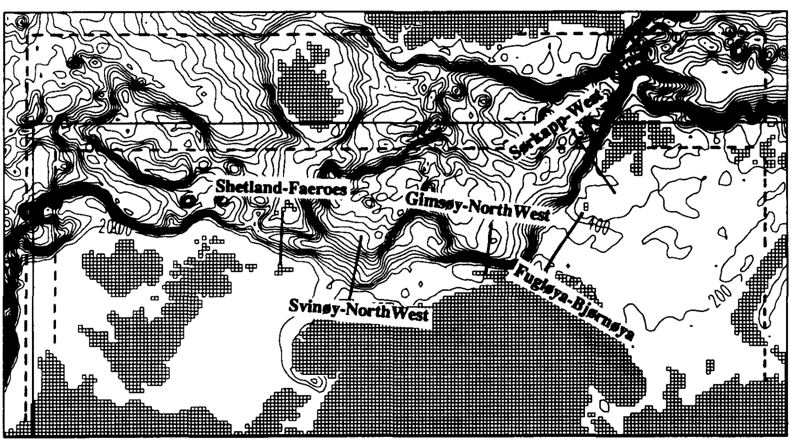


*Fig. 1.* Model domain and bathymetry for the standard run (SR) and the reduced domain which was used in the sensitivity tests (Subsection 5.2.2). The depth contours are drawn for every 200 m. The FRS zones for the two domains are indicated by dashed lines. The locations of the five selected cross sections are also shown.

However, to be able to compute the velocities $u$ and $v$, we must first determine the depth mean velocities $u_m$ and $v_m$, or the transports, in the FRS zones at the open boundaries. Determining transports at the open boundaries of a model domain has always been a demanding task for oceanographic modellers dealing with limited area models. However, by using the FRS as open boundary condition, a rather simple approach may be utilized, at least for *diagnostic* climatological simulations.

In general, the transports at open boundaries are difficult to determine because of sparse and insufficient data. For climatological, and especially diagnostic simulations, a near stationary circulation (or solution) will eventually be obtained, which is representative for a given time or period. For a limited ocean area, a stationary solution requires zero net transports integrated along the open boundaries. Thus, to maintain a stationary circulation, the inflow into the model domain must continuously be compensated by an equal outflow. One obvious way to achieve zero integrated transport is simply to put the transport itself equal to zero *everywhere* at the open boundaries. Because of the properties of the FRS, this rather artificial boundary condition will be redistributed in a realistic way to nonzero transports through the FRS zones. This is because the FRS does not conserve mass or momentum. With decreasing $\alpha$ through these zones the dynamical equations (interior solution) will increase their control over the circulation. Several tests have shown that nonzero transport exists within the FRS zones although the external solution at the outer edge of these zones is specified as zero transport.

The motivation for choosing zero transports at the open boundaries is only to make things easy since we do not know the exact transports at the open boundaries. Coupled with the ability of the FRS to "transform" zero transport to nonzero through the FRS zones, this in fact produces a *reasonable* boundary condition for transport, at least for *diagnostic* simulations. However, the transformation from zero to nonzero transports by the FRS might often be insufficient to produce proper boundary conditions, and thereby causing an unacceptable difference between the external and internal solutions, especially in dynamically active areas. Also, for *prognostic* simulations zero transports are of course not recommended as boundary condition. In this case, boundary values should be extracted from diagnostic simulations on a larger domain.

By using the very simple constraint of $u_m = v_m = 0$ everywhere for the external solution in the FRS zones, the velocities $u$ and $v$ can be calculated from (4.3) and (4.4) in the entire model domain, also including the FRS zones. The computed velocity at 10 m depth, based on the climatological density field for February and the constraint of zero depth mean current, is shown in Fig. 2.

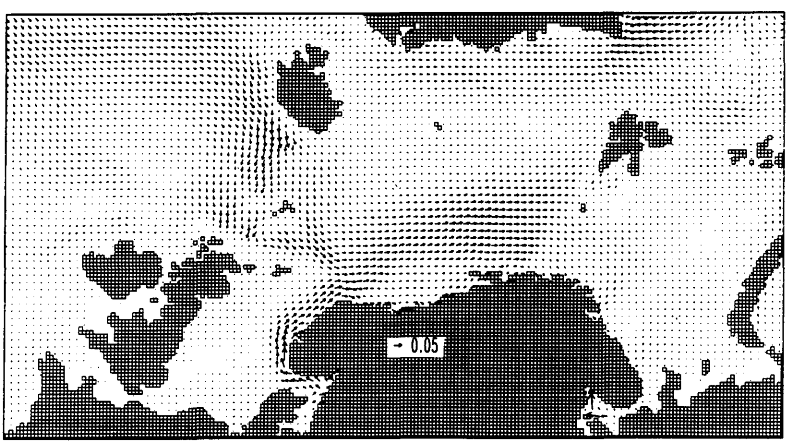


*Fig. 2.* Velocity field ($ms^{-1}$) at 10 m depth computed from the climatological density field valid for February. Arrows are drawn for every second grid point.

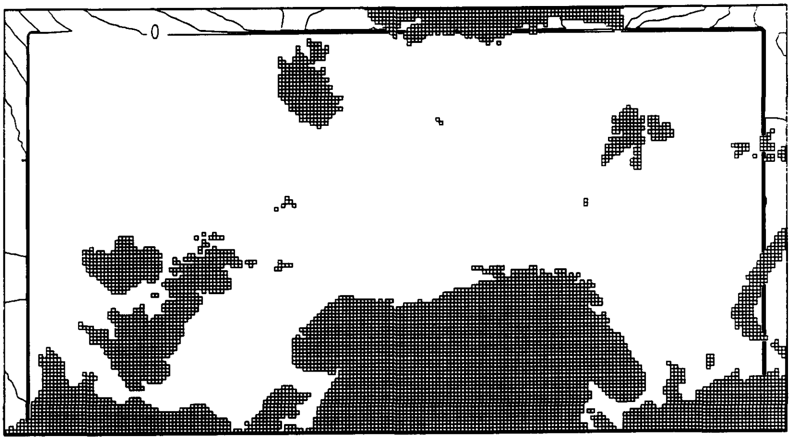


*Fig. 3.* Sea surface elevation computed from the climatological density field valid for February. Contour interval is 0.04 m.

The second parameter to be determined at the open boundaries, or in the FRS zones, is the sea surface elevation $\eta$. First, the gradient of $\eta$ is computed from geostrophic balance using the velocities in the upper level (i.e., the velocities representative for the upper discrete layer). Then, $\eta$ itself is computed by numerical integration performed along the boundaries of the model domain. Since the east coast of Greenland is a part of the model domain, and divides the southern and northern open boundaries, see Fig. 1, computation of $\eta$ was also performed *along* the coast of Greenland where, of course, the transport perpendicular to the coast is zero. By this procedure, the boundary value of $\eta$ south of Greenland became different from the boundary value north of Greenland. Note that values for $\eta$ were only computed within the FRS zones.

In the same way as for the velocities, we have to determine an integration constant. Concerning the numerical integration, this is the value of $\eta$ in the "first point of calculation", which was chosen to be the lower left-hand corner of the model domain depicted in Fig. 1. Since the gradient of the sea surface elevation is directly determined from the velocities in the upper level, we expected the computed gradient of $\eta$ in the FRS zones to reflect a "correct" pressure gradient connected to the velocity pattern in the upper level. Regarding Fig. 2 showing the velocities at 10 m depth, there is *inflow* almost everywhere along the open boundaries. This should then be reflected in the sea level as a more or less steady *decrease* from the value in the "first point of calculation". Indeed, the computed sea level in the FRS zones showed a relatively smooth decrease from the chosen value in the "first point of calculation" to the last computed value in the lower right-hand corner of the model domain, i.e., on the Siberian Shelf. The resulting sea surface elevation is shown in Fig. 3. In this study we have chosen the value of the integration constant to be equal to half the *positive* value of $\eta$ in the "last point of calculation". From several tests, the choice of this integration constant only affects the height of the sea level, not the gradients and thereby the transports.

## 5. The numerical experiments

### *5.1. The standard run (SR)*

The first simulation was performed to get results from a reference or "Standard Run". The results from the different test runs may then be compared with the results from this Standard Run, hereafter denoted SR. In fact, the setup for the SR was almost identical to the setup for the simulations which were performed to produce The Diagnostic Archive. The model domain for the SR is shown in Fig. 1. It covers the Greenland and Norwegian Seas, parts of the North East Atlantic and the Arctic Ocean, together with the North Sea and

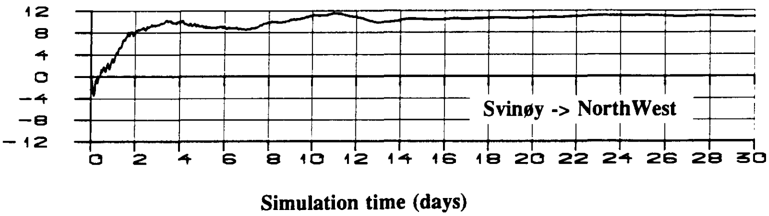


*Fig. 4.* Time series of net northward fluxes (in Sverdrup) through the vertical cross-section Svinøy-Northwest (see also Fig. 1).

the Barents Sea. Three open boundaries exist. The fourth boundary is closed by the European coast. The model grid has a horizontal resolution of 20 km, and the model domain consists of 218 times 120 horizontal grid points. In the vertical 10 $\sigma$-levels were used. In a depth column of 1000 m, the $\sigma$-levels are situated at 0, 2, 10, 75, 150, 300, 500, 700, 950 and 1000 m. Thus, for a depth of 100 m, the $\sigma$-levels are 0 m, 0.2 m, 1.0 m, 7.5 m etc. The time step was 600 s (10 min) for the internal mode, and 20 seconds for the external mode. In the Smagorinsky formulation of the lateral eddy viscosity in (2.8), the coefficient $C$ was set equal to 0.1. The vertical eddy viscosity coefficient were computed by using the second order turbulence closure sub-model (Mellor and Yamada, 1982). The Coriolis parameter $f$ was computed in each grid point, $f = 2\Omega \sin \Phi$, where $\Omega = 7.292 \times 10^{-5}\ \mathrm{s}^{-1}$ is the earth's angular velocity, and $\Phi$ is the latitude. The gravitational acceleration $g = 9.806\ \mathrm{ms}^{-1}$.

The only forcing or input to the model consisted of the gridded climatological fields of salinity and temperature for *February*. Based on these fields, the model computes a density field by the equation of state (2.5). Boundary values for the current velocities and the sea surface elevation were computed as described in Section 4. By using the FRS, values of sea level and current produced by the model were relaxed towards these specified boundary values within the FRS zones. The width of the relaxation zones was seven grid points or 120 km. Since it was possible to determine the thermal wind component of the current *everywhere* in the model domain from the initial density field, the computed non-zero velocities (see Fig. 2) were also used as initial values for the current. As mentioned in Section 4, values for the sea surface elevation were only computed in the FRS zones. Otherwise, in the interior model domain, the sea surface elevation was initially zero. Earlier simulations have

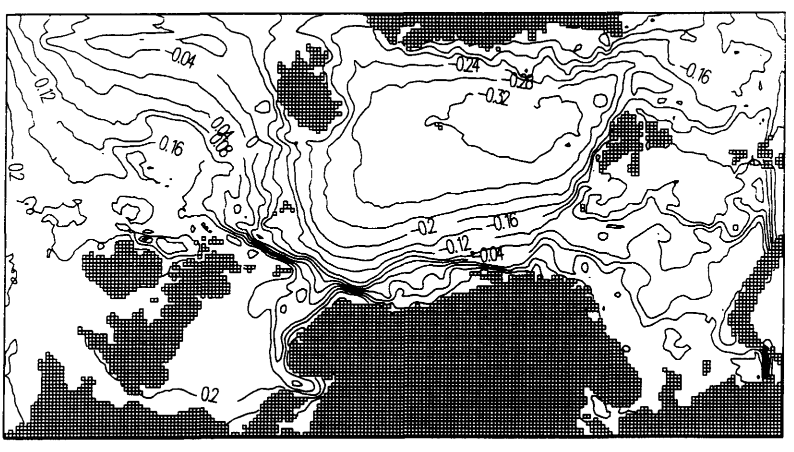


*Fig. 5.* Sea surface elevation after 30 days of simulation from the standard run. Contour interval 0.04 m.

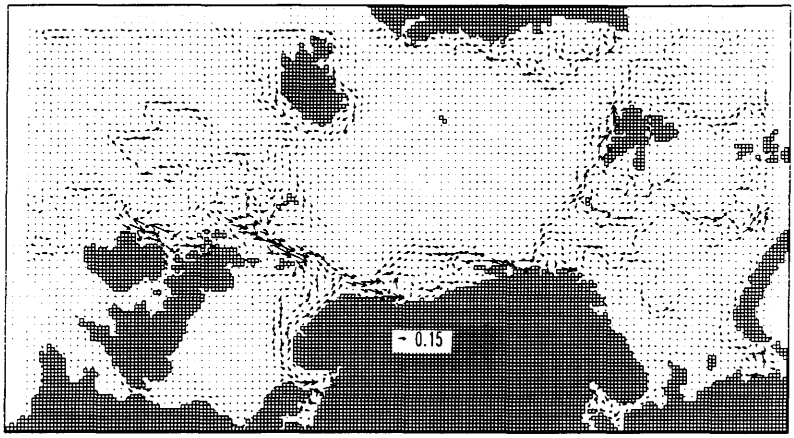


*Fig. 6.* Depth mean current (ms $^{-1}$) after 30 days of simulation from the standard run. Arrows are drawn for every second grid point.

shown that starting with nonzero instead of zero initial current in the interior model domain, has no influence on the model results. This is also the case regarding the sea level, as long as it is specified to a *constant* value in the interior model domain.

The model was run in diagnostic mode until a stationary or near stationary circulation was obtained. This was controlled by inspection of time series of *net northward fluxes* through five selected vertical cross-sections along the European Shelf; see Fig. 1. An example for the section Svinøy-NorthWest is shown in Fig. 4. From this figure, a near stationary solution was obtained after approximately 15 days of simulation. Thus, it should be reasonable to regard the computed circulation after 30 days of simulation as a stationary solution.

The sea surface elevation after 30 days is shown in Fig. 5, and the associated depth mean current in Fig. 6. The current at 10 m depth after 30 days is shown in Fig. 7. From the figures we see that some of the well known large scale features in the ocean circulation are also present in the model results. The Norwegian Atlantic Current flows in between Shetland and the Faeroes, and follows the Norwegian shelf break north to Tromsøflaket

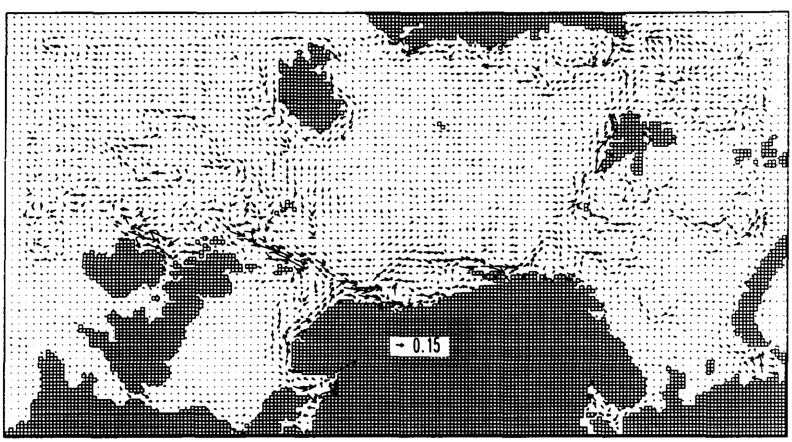


*Fig. 7.* Current (ms $^{-1}$) at 10 m depth after 30 days of simulation from the Standard Run. Arrows are drawn for every second grid point.

where it splits into two branches, one into the Barents Sea, and the other flowing further northward along the slope west of Spitzbergen. The East-Greenland current and the anticyclonic (clockwise) circulation around Iceland are also present in the results from this simple diagnostic run. However, the model produces only one large cyclonic (counter clockwise) gyre in the Nordic Seas, not the observed two gyres associated with the separate Norwegian and Greenland basins. One reason for this may be that the underlying bottom topography is not reflected in the rather smooth hydrographical driving fields. In addition, there was no wind forcing present in this simulation.

The current in the southwest Barents Sea fits the observed features quite well. In particular the topographic effect of Tromsøflaket is very pronounced. However, further north and east, and thereby closer to the open boundaries, the model current shows no sign of the Polar Front, and passes more or less straight through and leaves the Barents Sea between Novaya Zemlya and Franz Josef Land. The observed Arctic Water that flows south and west in the Barents Sea is not found in the model results. This is to a large extent due to the fact that the density field associated with the Polar Front is not present in the applied climatological data of salinity and sea temperature. Also, the boundary values in this area are most likely poor. Earlier experience has revealed that the interior solution is affected by the boundary values over a width of approximately two FRS zones inside of the open boundaries. The North Sea model circulation is better. This is mainly due to the more detailed climatology from Damm (1989) which was applied in this area. There is a reasonable in- and outflow in the Norwegian Trench. Also the Norwegian coastal current is visible. However, this current is lost further north where the density field is more smooth. The net northward fluxes produced by the model after 30 days of simulation for the five selected vertical cross-sections along the European Shelf shown in Fig. 1, are presented in Table 1 below.

The values in Table 1 compare well with values from the literature; see for instance Worthington (1970), Gould et al. (1985), McClimans (1991, private communication). The difference between the Svinøy section and the Shetland-Faeroes channel further south may be due to Atlantic Water flowing in west of the Faeroes, and to internal circulation in the Nordic Seas. Fig. 8 shows vertical cross sections of velocity for two of the five sections in Table 1. From this figure we see that the strongest flow is situated over the continental shelf break.

Table 1. *Net northward fluxes in Sverdrup after 30 days of simulation*

| Cross-section | Fluxes in Sverdrup |
|---|---|
| Shetland → Faeroes | 6.1 |
| Svinøy → NorthWest | 10.9 |
| Gimsøy → NorthWest | 10.2 |
| Fugløya → Bjørnøya | 2.8 |
| Sørkapp → West | 12.0 |

The overall impression from the results is that the model circulation, to a large extent, seems to be *depth independent*. This is in agreement with the results both from Legutke (1991) and Stevens (1991), although they also applied atmospheric forcing. The vertical cross section plots of velocity in Fig. 8 (almost vertical isolines) reflect the behaviour of nearly depth independent flow. Thus, the flow is strongly steered by the topography. The model circulation is a result of the forcing from the imposed climatological density field. This circulation turns out to be quite sensitive to the specification of the *sea level* at the open boundaries.

The results from the SR show that the model with the FRS as open boundary condition and with boundary values for sea level and current velocities computed as described in Section 4, produces a reasonable circulation, at least for the interior model domain (i.e., The North Sea and the Nordic Seas), even when the only forcing is provided by the climatological density field.

### 5.2. *Sensitivity tests*

*5.2.1. Specifications at the open boundaries.* The circulation pattern which was produced by the SR, and described in the previous section, is a result of *both* the imposed density field in the entire model domain, and the specified velocities and sea level at the open boundaries. To study the sensitivity due to different specifications of sea level and currents at the open boundaries, a run was performed in which both sea level and velocities were put equal to zero everywhere along the open boundaries, i.e., the external solutions for sea level

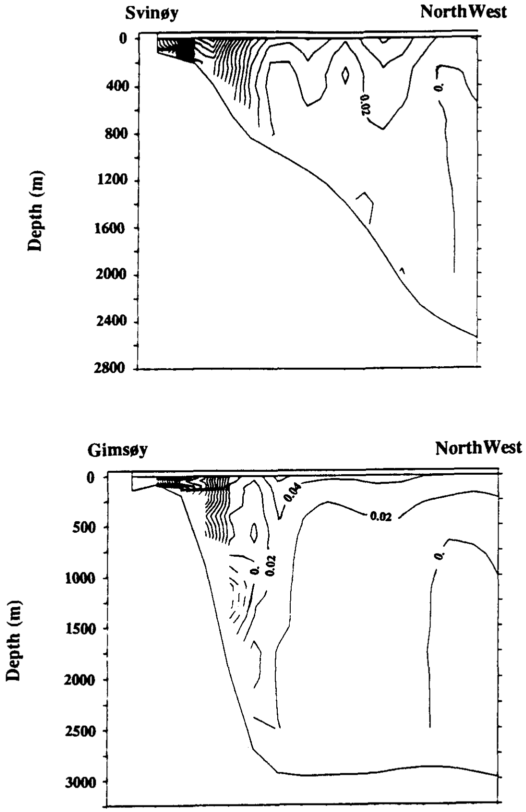


*Fig. 8*. Vertical cross-sections of velocity from the Standard Run for two of the five selected sections (see Fig. 1). Contour interval is 0.02 $ms^{-1}$. Dashed contour lines indicate "southward" flow.

and current were equal to zero in the FRS zones. Otherwise, the set up was as in the SR.

Because of the zero boundary conditions for both sea level and current, the circulation produced by the model in this case is driven mainly by the imposed climatological density field. The depth mean currents after 30 days are shown in Fig. 9. Some of the large scale features in the Nordic Seas circulation may still be recognized, like the clockwise circulation around Iceland, the slope current along the Greenland Shelf, and the slope current along the shelf between Norway and Spitzbergen with signs of the branching of the current into the Barents Sea at Tromsøflaket. However, the Atlantic inflow between Iceland and Scotland, especially in the Shetland-Faroes channel, together with the flow along the Norwegian Shelf, are poorly simulated. The flow pattern is rather noisy, and actually indicates a *southward* flow along the Norwegian Shelf.

Thus, the change of specifications at the open boundaries clearly has a strong influence on the circulation produced in the interior of the model domain. The specification of zero sea level and velocities (in addition to zero transport) must be regarded as a highly unrealistic and incorrect boundary condition. The poor circulation which was produced by the model in this case should therefore be no surprise. On the other hand, with zero transport but nonzero sea level and velocities at the open boundaries, the model produced a satisfactory circulation in the SR, at least in the Nordic Seas, even though specification of zero transport at the open boundaries is also an artificial and unrealistic boundary condition.

Returning to the results from the SR, we only established that the model produced a satisfactory circulation in the *interior* model domain, far away from the open boundaries. Because most of the available data, such as volume fluxes, only existed for the European Shelf reaching from west of Scotland north to Spitzbergen, it was natural to compare the model results with observed values in these areas. However, as was also pointed out in the discussion of the results from the SR in Subsection 5.1, the model performed poorer in the eastern Barents Sea, which is an area situated rather close to an open boundary.

Second, the model results from the SR showed that the circulation is strongly steered by topography. In fact, both Legutke (1991) and Stevens (1991) state that the circulation in the actual area to a large degree follows contours of $f/H$, which is also seen in our results. Because of this, it is especially important to specify "correct" transports at the boundaries where the $f/H$ contours enter or leave the model domain, see for instance Greatbatch and Goulding (1992). In the Nordic Seas, the contours of $f/H$ are mostly *closed* within the model domain, except for a narrow passage between Spitzbergen and Greenland. Together with the ability of the FRS to redistribute the applied zero transports to nonzero within the FRS zones, the closed $f/H$ contours makes it possible for the model to set up a satisfactory circulation in the Nordic Seas.

Test runs in which only the sea level was nonzero at the open boundaries, gave results com-

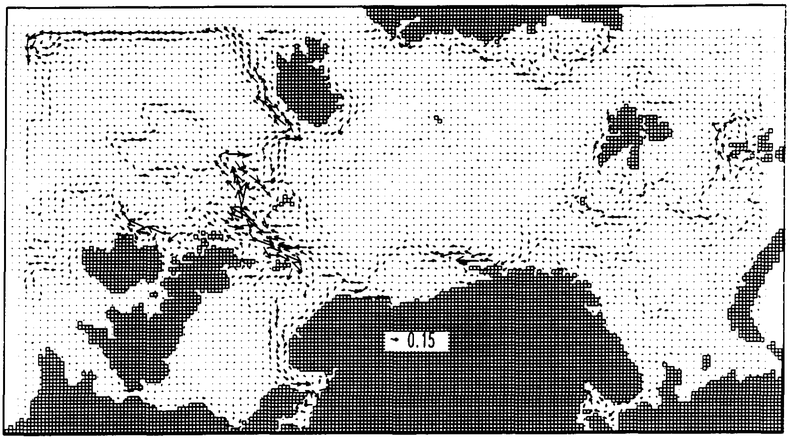


*Fig. 9.* Depth mean current ($ms^{-1}$) after 30 days of simulation with zero sea level and velocities at the open boundaries. Arrows are drawn for every second grid point.

parable to those from the SR where both sea level and velocities were specified as nonzero in the FRS zones at the open boundaries. Other tests with zero sea level and nonzero velocities gave a quite different result when compared with the SR. The reason for this may be found in the model equations. The specified volume fluxes in the FRS zones have almost zero divergence. Thus, the contribution to the sea surface elevation through the continuity equation is very small. Then, in the momentum equations the only contribution (except bottom friction and viscosity) is from the non-linear convective terms (specification of velocity in one direction excludes the Coriolis term as well). By this procedure, the energy input is rather small, and the solution will consist of a much weaker circulation. On the other hand, with non-zero sea surface elevation and zero velocities, the pressure gradient in the momentum equations will contribute (even with a constant sea level in the FRS zones as long as it *differs* from the initial sea level in the rest of the model domain) to put a lot more energy into the solution than is possible by the convective terms.

Since the sea surface elevation at the open boundaries seems to be the most sensitive parameter regarding the model produced circulation, this also opens the possibility to actually control the strength of the circulation by simply changing the sea level at the boundaries. This was indeed demonstrated in Engedahl (1992).

Thus, we may conclude that by applying the FRS at the open boundaries, it is possible to easily *construct* open boundary conditions which should set up a reasonable circulation within the model domain. Here, the crucial parameter is the sea surface elevation. Experiments have revealed that the strength of the circulation may be controlled by specifying an *additional* sea level difference at the open boundaries (Engedahl, 1992). However, the success of the model in simulating the circulation in the Nordic Seas was caused partly by the fact that this area is situated rather far away from the open boundaries, and partly by the existence of *closed* $f/H$ contours in that area. It is not likely that the model will manage to produce an equally satisfactory circulation if the $f/H$ contours leave or enter the model domain, and when an unrealistic transport (like zero) is specified at the open boundaries. This is further studied in Subsection 5.2.2.

*5.2.2. Choice of location of the open boundaries and specification of the boundary values.* Relative to the model domain in the SR, the model area was reduced by 8 grid points in the south, and in westerly direction the extension was reduced from 120 to 89 grid points. The reduced domain is shown embedded in the domain for the SR in Fig. 1. Otherwise, the set up was as in the SR. In this reduced model domain, the open boundary in the west is now situated so that only about half the ocean basin (Greenland and Norwegian Basins) in the Nordic Seas is included in the

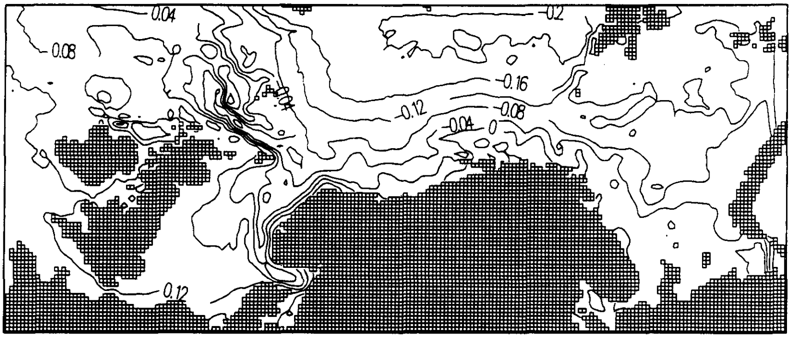


*Fig. 10.* Sea surface elevation after 30 days of simulation with the reduced model domain when the boundary values are computed as described in Section 4. Contour interval 0.04 m.

model. Thus, in *this* case, most contours of $f/H$ leave or enter the model domain.

(*a*) *Boundary values computed as described in Section 4*

The boundary values were computed with the same constraint of zero transports everywhere, as was performed for the SR. As in the SR, the initial climatological current in the interior model domain was derived from the thermal wind equations. Sea surface elevation and depth mean currents after 30 days of simulation are shown in Fig. 10 and 11, respectively. If we had been able to apply "perfect" open boundary conditions, the results in Fig. 10 and 11 should have been almost identical to the results for a segment in Fig. 5 and 6 covering the same area. However, Fig. 10 and 11 depict a quite different circulation than that from the SR in Fig. 5 and 6.

Regarding the depth mean current, a rather noisy and chaotic behaviour is observed, as for instance in the Shetland-Faroes channel. Fig. 11 also shows signs of a *southward* flow along the Norwegian Shelf. Actually, the results now look more like the results described in Subsection 5.2.1, where zero sea level and velocities were applied at the open boundaries of the large domain; see Fig. 9. The results from that run was considered to be rather poor, and that must also be the conclusion regarding the results from this run with the reduced model domain.

Thus, the effects of moving the area of interest (the Nordic Seas) closer to the open boundaries (or vice versa), and specifying imperfect boundary

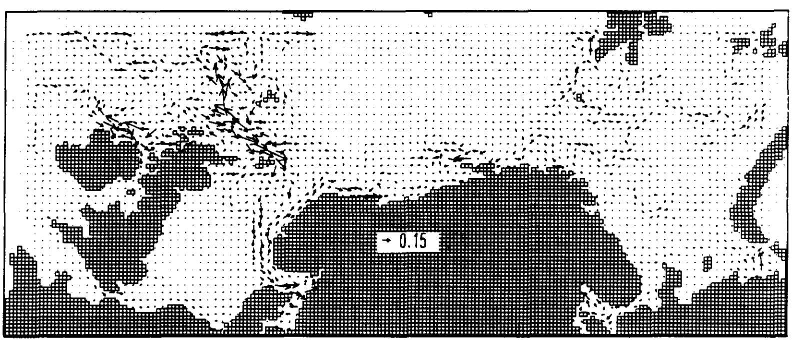


*Fig. 11.* Depth mean current ($ms^{-1}$) after 30 days of simulation with the reduced model domain when the boundary values are computed as described in Section 4. Arrows are drawn for every second grid point.

conditions or external solutions where the $f/H$ contours reach the boundaries, have substantial influence on the results in the model domain. Even though the FRS always will try to redistribute zero transports to nonzero through the FRS zones, this was not sufficient to compensate the artificial boundary condition in this case.

Fortunately, we have the "perfect" boundary values or external solutions for sea level and current (in dynamic balance) available in the results from the SR. The FRS was originally designed as a one-way influence nesting technique for relaxing solutions from a large model into a smaller model domain. It should therefore be able to perform well when the boundary values or external solutions originate from the SR instead of being computed as outlined in Section 4.

*(b) Boundary values from the standard run (SR)*

A second test run with the same reduced model domain, but now with boundary values of sea level and current obtained from the results of the SR, was performed. Note that in this run the initial values for *both* sea level and current were zero in the interior model domain. Comparing the results with the results from the SR, we now find almost exactly the same circulation. This is clearly seen in Fig. 12 which depicts the sea level after 30 days from this run (heavy contour-lines) plotted on top of the sea level from the SR. Thus, as stated by Martinsen and Engedahl (1987), the FRS will always show an excellent performance, provided that reasonable boundary values or external solutions are available.

*5.3. An example from a prognostic simulation*

As already mentioned the presented study arose from the work of creating climatological archives containing sea level, current, salinity and temperature. Two archives were produced. First, a *Diagnostic Archive* with monthly mean fields of sea level and current. This archive was produced by running the model in diagnostic mode with simple boundary conditions for sea level and current as in the SR. A *Prognostic Archive* containing monthly mean fields of sea level, current, salinity and temperature was produced by running the model in prognostic mode for several years. During this simulation both salinity and temperature were allowed to evolve. In addition, the model was also forced by monthly mean winds and fresh water discharge, and the $M_2$ tide was applied. The model domain for The Prognostic Archive was smaller than the domain for The Diagnostic Archive. Thus, boundary values for sea level and current were taken from The Diagnostic Archive and used as external solutions in the FRS.

An example of the current at 10 m for May from The Diagnostic Archive is shown in Fig. 13. Fig. 14 shows the same current from The Prognostic

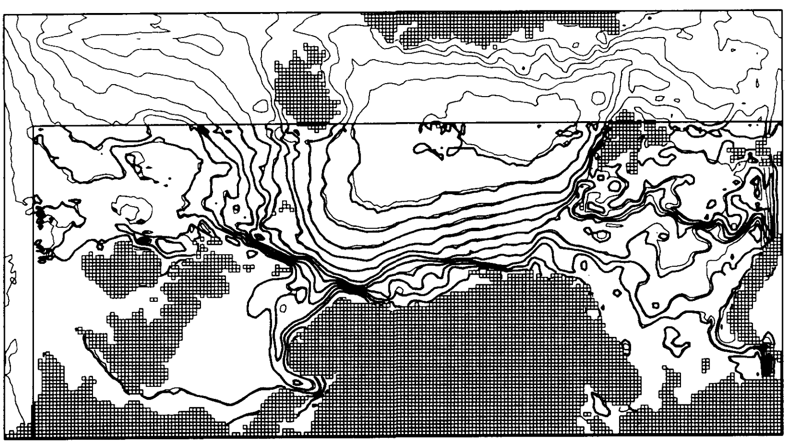

*Fig. 12.* Sea surface elevation after 30 days of simulation with the reduced model domain when the boundary values are extracted from the solution in the standard run (bold contour lines), together with the sea level computed in the Standard Run. Contour interval 0.04 m.

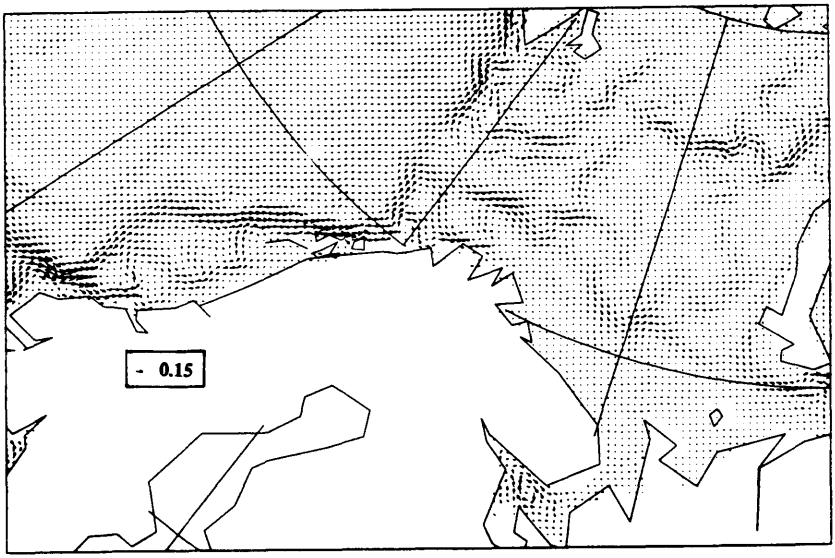


*Fig. 13.* Current ($ms^{-1}$) at 10 m depth from *The Diagnostic Archive.* Arrows are drawn for every grid point.


*Fig. 14.* Current ($ms^{-1}$) at 10 m depth from *The Prognostic Archive.* Arrows are drawn for every grid point.

Archive. In the results from The Prognostic Archive the northward flow over the deep areas off the continental slope near the coast is more pronounced. Also, the large scale eddies on the Norwegian Shelf are more developed. For further results, see Martinsen et al. (1992).

## 6. Summary and conclusions

In this paper, we have focused on the performance of the Flow Relaxation Scheme (FRS) as open boundary condition in *diagnostic* simulations where salinity and temperature are kept constant in time. The model was run until a stationary solution was obtained. The only interior forcing was provided by gridded climatological fields of salinity and temperature, originating from Levitus (1982) and Damm (1989). In addition, the model was driven by the specifications of sea level and currents at the open boundaries.

A simple method for determining boundary values of sea level and currents was outlined. Based on the available climatological density field, the thermal wind components of the current were computed in each level with the condition of zero depth mean current (or transport) everywhere. This is of course an artificial open boundary condition in a limited area model, especially if it is applied in dynamically active areas where contours of $f/H$ enter or leave the model domain. However, if the area of interest is not situated very close to the open boundaries and if it contains mostly closed contour lines of $f/H$, the model produces a satisfactory circulation in the actual area. This is because the FRS will always try to redistribute zero transports to nonzero in a realistic way through the FRS zones. If the open boundaries are not situated in areas with strong inflow or outflow, the redistributed nonzero transports might be sufficient to establish reasonable boundary conditions.

The choice of zero transports at the open boundaries is a consequence of the fact that the transports at the boundaries of a realistic model domain are usually poorly known, and available estimates are often uncertain. Of course, if any reliable estimates of the transports are available, they should be used as external solutions when the FRS is applied. The latter was clearly demonstrated by applying the model to a section of the original model domain, and by using the computed sea level and currents from the whole domain as external solutions at the open boundaries. Because the FRS was originally designed as a one way influence nesting technique, this gave excellent results. We obtained almost exactly the same circulation as was produced in the large domain.

The model with the FRS as open boundary condition has also shown satisfactory results in *prognostic* simulations including atmospheric forcing, tides and fresh water discharge from the main European rivers and the Baltic (Martinsen et al., 1992). Here, the boundary values, or external solutions for sea level and current were extracted from the results for a larger domain, where the model was run in diagnostic mode and with a setup similar to that for the Standard Run (SR). An example of the results from a prognostic simulation was given in Subsection 5.3. It showed that the FRS works well also when the temperature and salinity fields are allowed to evolve.

## 7. Acknowledgements

The author likes to thank both Dr. Eivind A. Martinsen and Professor Jan Erik Weber for many useful discussions during this work, together with valuable suggestions for the manuscript. The presented study was supported by NAVF, the Norwegian Research Council for Science and the Humanities, and partly by the OKN (Operation Committee North)-group consisting of oil companies being operators on the Norwegian Shelf north of 62° N.

## REFERENCES

Blumberg, A. F. and Mellor, G. L. 1987. A description of a three-dimensional coastal ocean circulation model. *Three-dimensional Coastal Ocean Models*, **4**, (ed. N. Heaps), American Geophysical Union, Washington DC, 208 pp.

Cooper, C. K. and Thompson, J. D. 1989. Hurricane generated currents on the outer shelf. 2: Model sensitivity studies. *J. Geophys. Res.* **94-C9**, 12540–12554.

Damm, P. 1989. Klimatologischer Atlas des Salzgehaltes, der Temperatur und der Dichte in der Nordsee, 1968–1985. *Techn. Report 6-89.* Institut fur Meereskunde, University of Hamburg, Germany.

Davies, H. C. 1976. A lateral boundary formulation for multi-level prediction models. *Quart. J. Roy. Meteor. Soc.* **102**, 405–418.

Davies, H. C. 1983. Limitations on some common lateral boundary schemes used in regional NWP models. *Mon. Wea. Rev.* **11**, 1002–1012.

Engedahl, H. 1992. Specification of boundary values and use of the flow relaxation scheme in a three-dimensional ocean model. Institute of Geophysics, University of Oslo. *Institute Report Series no. 83*, 63 pages.

Gould, W. J., Loynes, J. and Backhaus, J. 1985. Seasonality in slope current transports NW of Shetland. *ICES Paper from annual meeting 1985/ section C*, paper no. 7.

Greatbatch, R. J. and Goulding, A. 1992. A long-time scale, density stratified shelf circulation model. *Cont. Shelf Res.* **12**, 115–141.

Hannah, C. G., Leblond, P. H., Crawford, W. G. and Budgell, W. P. 1991. Wind-driven depth-averaged circulation in Queen Charlotte Sound and Hecate Strait. *Atmosphere-Ocean* **29**, 712–736.

Kållberg, P. and Gibson, J. K. 1977. Lateral boundary conditions for a limited area version of the ECMWF model. *WMO, Geneva, WGNE Progress Report no. 14*, 103–105.

Legutke, S. 1991. A numerical investigation of the circulation in the Greenland and Norwegian Seas. *J. Phys. Oceanogr.* **21**, 117–148.

Levitus, S. 1982. Climatological Atlas of the World Ocean. *NOAA Professional Paper 13.* US Dept. of Commerce, Washington DC, 173 pp.

Martinsen, E. A., Engedahl, H., Ådlandsvik, B., Ottersen, G., Loeng, H. and Balino, B. 1992. MetOcean MOdeling Project: Climatological and hydrographical data for hindcast of ocean currents. *Technical Report no. 100.* The Norwegian Meteorological Institute, Oslo, Norway.

Martinsen, E. A. and Engedahl, H. 1987. Implementation and testing of a lateral boundary scheme as an open boundary condition in a barotropic ocean model. *Coastal Engineering* **11**, 603–627.

Mellor, G. L. and Yamada, T. 1982. Development of a turbulence closure model for geophysical fluid problems. *Rev. Geophys. Space Phys.* **20**, 851–875.

Smagorinsky, J. 1963. General circulation experiments with the primitive equations, I. The basic experiment. *Mon. Weather Rev.* **91**, 99–164.

Stevens, D. P. 1991. A numerical ocean circulation model of the Norwegian and Greenland Seas. *Prog. Oceanog.* **27**, 365–402.

Worthington, L. V. 1970. The Norwegian Sea as a mediterranean sea. *Deep-Sea Res.* **17**, 77–85.